Structure of β-Isotactic Polypropylene: A Long-Standing Structural Puzzle‖

Stefano V. Meille,*,† Dino R. Ferro,‡ S. Brückner,§ Andrew J. Lovinger,⊥ and Frank J. Padden⊥

Dipartimento di Chimica, Politecnico di Milano, via Mancinelli 7, 20131 Milano, Italy, Istituto di Chimica delle Macromolecole, CNR, via Bassini 15, 20133 Milano, Italy, Dipartimento di Scienze e Tecnologie Chimiche, Università di Udine, via del Cotonificio 108, 33100 Udine, Italy, and AT&T Bell Laboratories, 600 Mountain Avenue, Murray Hill, New Jersey 07974

Received August 5, 1993; Revised Manuscript Received November 19, 1993●

ABSTRACT: The structure of β-isotactic polypropylene (β-iPP) has been investigated taking into consideration X-ray and electron-diffraction data supplemented by packing energy calculations. The structure is characterized by extensive disorder, and two structural models can be envisaged: both are based on domains of helices all of the same chirality, arranged on a pseudohexagonal lattice. The simplest satisfactory model is trigonal ($P3_121$ and the enantiomorphic $P3_221$) with $a = b = 11.03$ Å and $c = 6.49$ Å. Three monomers form the asymmetric unit, and six chains, each with a 0.5 occupancy factor, coexist in the unit cell. This is a consequence of statistical directional disorder, just like in the α- and γ-crystalline modifications of isotactic polypropylene. Coupling of the chiral domains across (200) or ($\bar{2}$20) glide planes of the trigonal cell can result either in enantiomorphic twins or, if the domains are coherent, in a new achiral orthorhombic lattice with $a = 11.03$ Å, $b = 19.10$ Å, and $c = 6.49$ Å. The two models, which reasonably account for all the available experimental evidence concerning β-iPP, are only marginally different and can probably coexist. Preliminary packing-energy calculations confirm that both arrangements are acceptable. It is further suggested that similar structures based on incoherently or coherently coupled enantiomorphic domains of modest size are very likely in chiral crystalline polymorphs of achiral macromolecules.

Introduction

The determination of the crystal structures of α-[1] and γ-isotactic polypropylene (iPP)[2] was instrumental for the development of new ideas in the field of macromolecular science. The α-iPP crystal structure is connected with the establishment of the concept of stereoregularity and the recognition of its role as a prerequisite for polymer crystallization. Also, the idea of isosterism (i.e., closely similar steric requirements) of vinyl–polymer helices of the same chirality but opposite directionality is associated with the solution of the crystal structure of α-iPP.[1] On the other hand, the γ-iPP modification was the first polymer crystal structure for which an architecture based on nonparallel chains was established.[2] The full determination of the γ- and α-crystalline structures in the context of the overall polymorphic behavior of this polymer[3] has also been very fruitful in understanding the unique morphological features of iPP.[4–7]

A third crystalline phase of iPP (the β phase) was identified quite early by Keith and one of us,[8] but owing to its thermodynamic and mechanical instability,[3,8] it was never fully characterized, although a number of pertinent diffraction studies have been published.[3,8–13] These features, together with a substantially lower density[3] and a higher growth rate[8] as compared to the other crystalline iPP phases, are indications that high degrees of disorder must exist in this modification. The presence of peculiar streaks in the *hk*0 electron-diffraction patterns[11] confirms this conjecture and supports the idea that the full structural characterization of β-iPP could be helpful to specify disordered packing modes of iPP. All the available evidence indicates for this modification the same 3_1 helical conformation with a 6.5-Å repeat that is found in the α, in the γ, and in the mesomorphic phases of isotactic polypropylene. The question of whether the β-iPP packing may represent a suitable model for the arrangement of iPP chains in the mesomorphic phase of iPP is controversial.[14–19] We note that the issue is not a very clear one since no detailed packing and not even a convincing unit cell have been determined so far for β-iPP. More generally, since all the available evidence points to a modulation of an approximately hexagonal lattice in which each chain has six nearly equivalent nearest neighbors, it does appear reasonable that the β-iPP structure could enable a closer understanding of the highly disordered pseudohexagonal mesophases of helical macromolecules.

The experimental difficulties in the determination of the β-iPP crystal structure are substantial, as attempts to draw fibers of this modification cause the sample to transform to the mesomorphic phase and eventually to the more stable α-polymorph.[3] Furthermore, high proportions of β-crystallinity can be achieved only by melt crystallization either with the aid of certain heterogeneous nucleating agents,[20] by directional crystallization in a temperature gradient,[21,22] or again from melts subjected to shear.[23,24] In all these cases, however, the β-modification, due to its exceptionally low nucleation frequency as compared to α-iPP,[22] coexists with nonnegligible amounts of α-iPP. Considerable obstacles in the structural characterization of β-iPP are thus the simultaneous presence of other crystalline phases[3] and of disorder. The large nine-chain unit cell proposed by various authors[11,13] represents an additional difficulty.

Experimental Section

We have studied two different types of samples, all of them free of foreign nucleating agents. The first was crystallized in a temperature gradient of 200 °C/cm at a rate of 10 μm/min and resulted in a well-oriented sample of high β-iPP content.

† Politecnico di Milano.
‡ CNR.
§ Università di Udine.
⊥ AT&T Bell Laboratories.
‖ A preliminary communication on the subject was presented at the meeting XI Convegno Italiano di Scienze e Tecnologie delle Macromolecole, Sept 1993, Torino, Italy.
● Abstract published in *Advance ACS Abstracts*, February 1, 1994.

0024-9297/94/2227-2615$04.50/0

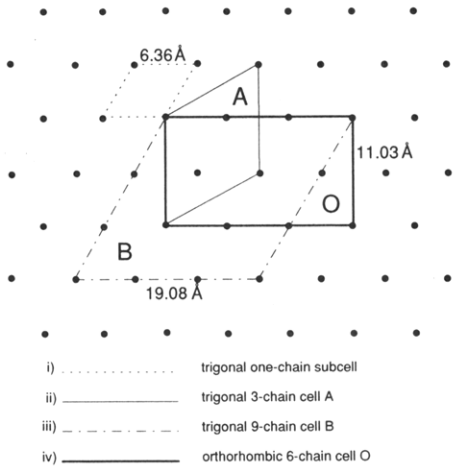

Figure 1. *c*-axis projections of the lattices discussed in the text: (i) trigonal one-chain subcell with a = 6.36 Å; (ii) trigonal cell A with a = 11.03 Å; (iii) trigonal cell B with a = 19.08 Å; (iv) C-centered orthorhombic cell O with a = 11.03 Å and b = 19.08 Å. The c axis has the same value of 6.49 Å in all lattices.

Surprisingly, substantial amounts of α were also present within regions that optically appeared to be pure β-iPP. In fact, a number of recent findings in the literature appear to suggest that some α-iPP can be included within β-iPP spherulites. Very weak mesomorphic diffraction maxima were also detectable in the X-ray diffraction patterns.

Samples suitable for electron diffraction were prepared by casting films from solution, melting them, and crystallizing them in a microscope oven under N_2 at various temperatures in the 120–136 °C range. In these samples, only small amounts of β-iPP were present, but very clear electron-diffraction patterns were obtained from selected regions of samples crystallized at 136 °C.

Electron-diffraction patterns were obtained at 100 kV using a JEOL 100CX transmission electron microscope in the selected area mode under low-irradiation conditions. The patterns were digitized using an Optronics Drum scanner and a bidimensional microdensitometer built by Officine Elettrotecniche di Tenno. X-ray diffraction patterns were recorded on a Statton vacuum camera with pinhole collimation using Ni-filtered Cu Kα radiation (40 kV, 25 mA) as well as on a Siemens D500 diffractometer using the same conditions already reported in ref 4.

Results and Discussion

All the published $hk0$ electron-diffraction patterns[10,11] and the available X-ray spectra of β-iPP[3,11-13] are characterized by one very prominent maximum with a d spacing close to 6.36 Å. As stated by Turner-Jones,[11] a substantial fraction of all the observed diffraction maxima, indeed comprising most of the more intense ones, can be accounted for by a hexagonal or trigonal lattice with $a = b$ = 6.36 Å and c = 6.49 Å (see Figure 1). As a consequence, this cell can be recognized as the basic subcell of the β-iPP structure: chains with a 3_1 helical symmetry are packed with their axes closely conforming to this lattice. All investigations in the more recent literature agree on this basic model, but difficulties arise if the additional reflections that do not fit the one-chain subcell are taken into due account: different lattices have been proposed, and no suggestion exists with respect to a possible space group. The two more detailed studies[11,13] agree in indicating a trigonal nine-chain unit cell with $a = b$ = 19.08 Å and c = 6.49 Å (cell B; see Figure 1). Some of the more prominent reflections that require the adoption of this lattice, e.g., the most intense with d = 6.26 Å (210), accidentally coincide with α-iPP spacings. On the other hand, in all the $hk0$ electron-diffraction patterns (see Figure 2) we obtained from iPP samples crystallized at 136 °C, all Bragg reflections could be indexed with the smaller trigonal (or hexagonal) unit cell with $a = b$ = 11.03 Å (cell A; see Figure 1) and there is not even the slightest indication of the above-mentioned equatorial reflections requiring lattice B.

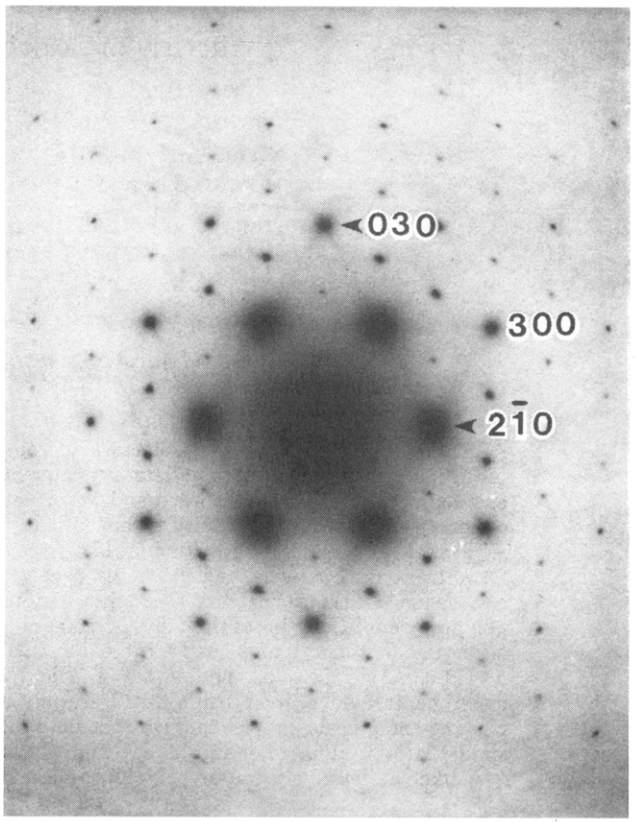

Figure 2. $hk0$ electron-diffraction pattern of β-iPP, hexagonal lamellae crystallized at 136 °C. The b^* axis is vertical (indexing with the trigonal A cell, Figure 1).

The A unit cell contains three instead of nine chains and had already been mentioned as an alternative, although unsatisfactory, possibility by Turner-Jones.[3,11] It had very reasonably been discarded by both that author and Samuels,[13] as it was inconceivable that samples which optically appeared to be single β-phase spherulites (commonly referred to as type 3 or type 4 spherulites) could also contain some α-iPP. However, we believe that this may have been the case: the X-ray diffraction pattern in Figure 3 which results from material obtained by oriented crystallization in a temperature gradient and which in the polarizing microscope appeared as pure β-modification, supports this idea (the area exposed to the pinhole-collimated beam is ca. 0.25 mm^2). It should be noted that the most prominent non-β-reflection, as expected at 6.26 Å, shows a *considerably lesser degree of orientation* than the β-phase reflections. This is consistent with the fact that some α-material is confined to very small domains, arising because of the much greater nucleation frequency of the α-phase but not developing to macroscopic dimensions because of the larger growth rate of the surrounding β-iPP. This can be demonstrated by polarizing optical microscopy from our directionally solidified specimens (see Figure 4). In Figure 4a, a low-magnification micrograph shows the oriented β-iPP matrix with transverse extinction bands due to the twisting of molecular orientation about the growth direction. Within this matrix, an α-iPP spherulite is clearly seen, having a teardrop shape as a result of its slower growth rate at this crystallization temperature.[22] A different region shown at much higher magnification in Figure 4b also contains a very small α-iPP spherulite which is almost undetectable because of over-

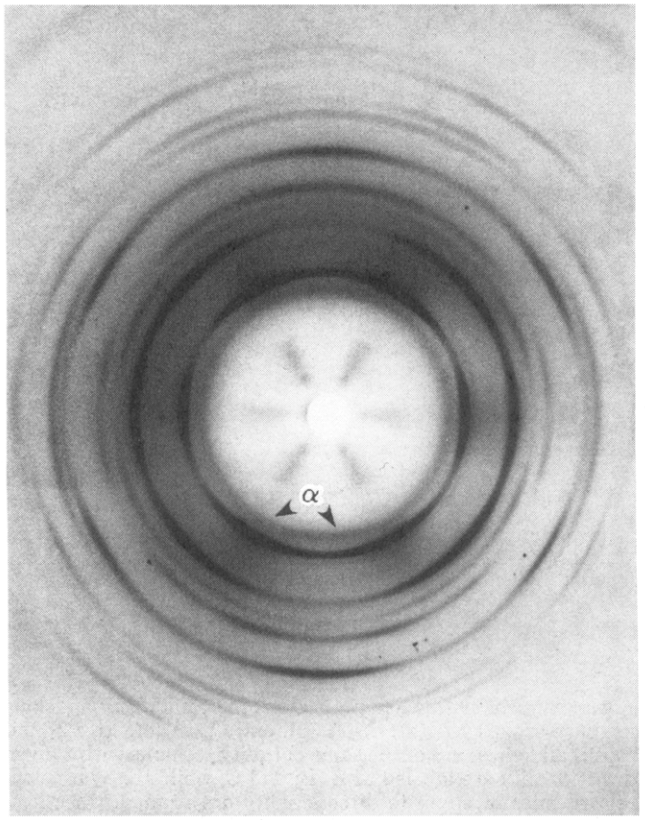

Figure 3. X-ray diffraction pattern from β-iPP unidirectionally crystallized in a temperature gradient. The b^* axis is vertical (A or O cell indexing, Figure 1) and corresponds to the temperature gradient, i.e., to the growth direction. Note that the innermost diffraction line (due to the α-modification) exhibits a substantially lower degree of orientation as compared to the other diffraction maxima.

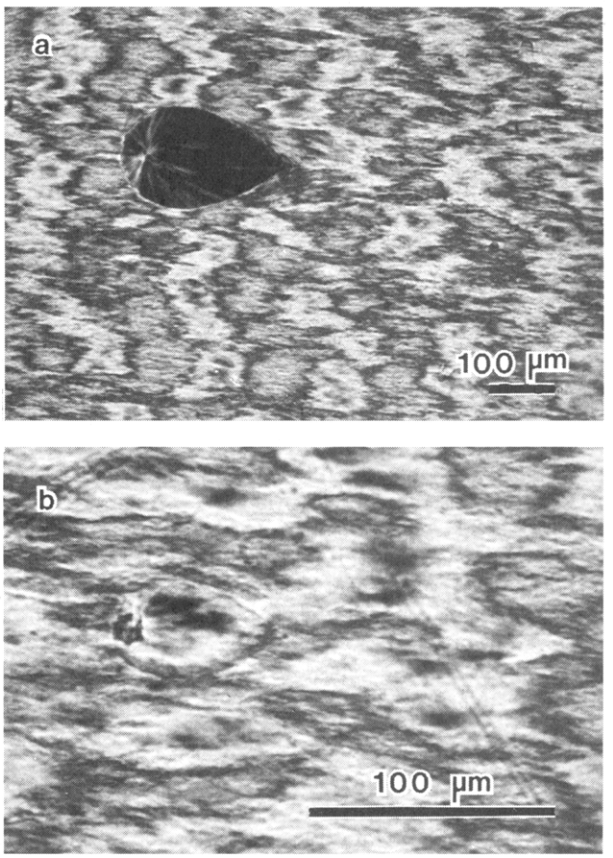

Figure 4. Polarizing optical micrographs of iPP unidirectionally crystallized at 10 °C/min in a 200 °C/cm temperature gradient. Growth direction is left to right. (a) Teardrop-shaped spherulite of α-iPP encapsulated within the faster growing β-iPP matrix. (b) Much smaller α-iPP spherulite, which is almost undetectable because of the overlapping featurs of the β-iPP matrix.

lapping banding from the oriented β-iPP matrix (to facilitate its observation it is located in the same position with respect to Figure 4b as its much larger counterpart is placed in Figure 4a).

Additional evidence results from diffractometer scans with samples with a surface area of 2–4 cm^2, again from unidirectionally crystallized films. These clearly show that the α-phase is inhomogeneously dispersed in the β-iPP matrix because, depending upon the sample orientation (i.e., exposed side, etc.), the α-component requires varying 0–corrections in some cases differing as much as 0.1° (2θ) from the one applicable to the coexisting β-iPP matrix. This is apparent from the fact that the separation between diffraction maxima is independent of sample orientation for diffraction maxima due to the same phase but may change substantially if the maxima are due to different phases (see Figure 5).

Consistent with the geometrical relationships among the various unit cells that can be taken into consideration (see Figure 1) and in order to comply with the 6.36-Å one-chain subcell, the helical axes of the three chains in the 11.03-Å hexagonal unit cell (A) have to be positioned at or very close to (0, 0), ($^1/_3$, $^2/_3$) and ($^2/_3$, $^1/_3$) in the x, y projection. A completely equivalent projection results assuming an orthorhombic c-centered lattice with a = 11.03 Å, b = 19.08 Å, and c = 6.49 Å, containing six chains in the unit cell placed respectively at (0, 0), (0, $^1/_3$) (0, $^2/_3$) and at the corresponding centered positions (O cell, Figure 1). We note that similar cells had already been proposed by Seto (according to ref 12) although the centering of the orthorhombic lattice was not specified. Disregarding intensity considerations, the reciprocal lattices of the A

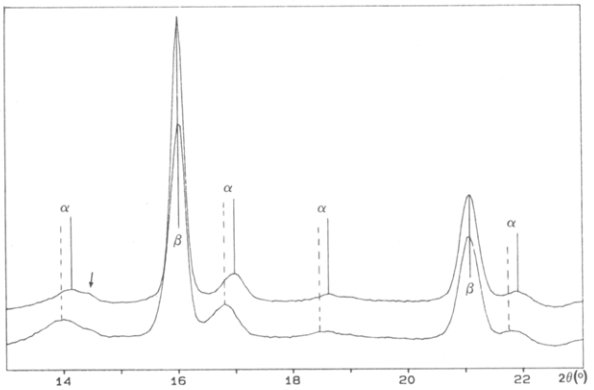

Figure 5. X-ray diffractometer patterns recorded from unidirectionally crystallized samples. The two patterns differ with respect to the orientation of the sample in the beam and suggest that the α-phase is largely located on one of the two film surfaces. Whereas the β-iPP diffraction maxima present, after appropriate zero correction, are of the same angular position, the figure clearly shows that different zero corrections must apply to the α-phase contribution. The arrow indicates a shoulder representing most likely diffraction due to mesophase impurities.

and of the O cells are geometrically equivalent, but symmetry and simplicity considerations suggest that it is preferable to work with the A cell unless substantial advantages can be envisaged. In fact, a centered orthorhombic cell implies extensive disorder as there are a minimum of 8 equivalent positions leading, with 3 independent chains in the asymmetric unit, to 24 chains in the unit cell. This lattice thus requires four chains each with an occupancy factor of 0.25 at each of the six

crystallographic sites (Figure 1, O cell). The final lattice choice is intimately related to the space group selected; this involves in turn a complete structural model, including a detailed description of disorder, which we can expect to be a major feature of this crystalline modification. Thus, the space group determination and the actual structural elucidation must proceed simultaneously.

In our investigation, we started from the simplest conceivable packing in cell A and proceeded by introducing increasing degrees of disorder as required by diffraction data. Rigorous 3_1 helices were treated in the rigid body approximation with their axial position fixed at (0, 0), ($^1/_3$, $^2/_3$), and ($^2/_3$, $^1/_3$), i.e., corresponding to ternary or hexagonal axes in trigonal and hexagonal space groups. The rhombohedral system could be excluded because reflection (111) should be systematically absent but is clearly observed (here and in the subsequent discussion, indexing will be given using lattice A unless otherwise indicated). The program LALS[25] was used throughout the electron-diffraction structural refinement. Indications from a projection using *hk*0 electron-diffraction data were sought in order to reduce the number of structural models to be investigated in detail. Six chains had to be used, two at each crystallographic position, as it was immediately apparent that three chains (one at each position) were unable to satisfactorily account for the observed *hk*0 intensities. Only the rotations around the chain axis were optimized considering models with different combinations of chain polarity (up–down). The intensity of primary spots (and specifically of reflection 110) should definitely cause double-diffraction. This will significantly affect diffracted intensities but will not result in the occurrence of prohibited reflections, as no *hk*0 systematic absences are apparent in the trigonal reciprocal lattice. Because of these effects, the results of the electron-diffraction analysis may need in the present instance to be tested against additional independent evidence.

Of the possible trigonal or hexagonal space groups, those with *p*3 and *p*6 projections are unsatisfactory because the observed symmetry of the *hk*0 pattern is higher than expected for these groups (for which $|F(hk0)| \neq |F(kh0)|$). All models characterized by centrosymmetric projections (i.e., the totality of pertinent hexagonal groups and a number of trigonal groups) or by projection symmetry *p*3*m*1 yield considerably poorer *R* discrepancy factors (typically 0.25–0.35 for 30 independent reflections) than models based on the projection symmetry *p*31*m* (*R* values as low as 0.10). We took that as a clear indication that it was unnecessary to pursue hexagonal space groups any further and that the projection symmetry was in fact *p*31*m*. Excluding space groups with simple ternary axes for obvious packing reasons and limiting the analysis to trigonal space groups with 3_1 axes, we were at this point left essentially with $P3_121$ (and with the enantiomorphic $P3_221$). Indeed, with this space group, satisfactory three-dimensional models fitting adequately the equatorial diffraction data could be obtained: six chains (three independent), each with occupation factor 0.5, are present in the unit cell. All helices are of the same chirality, and the structure is characterized by up–down statistical disorder similar but with interesting differences with respect to what is found in the α- and γ-modifications: notably, the methyl groups of "up" and "down" chains at each crystallographic position do not superimpose. As is apparent from Figure 6b, whereas the chains at position (0, 0) are symmetry related (A and A′), the chains that are symmetry-related to chains B and C′ at ($^2/_3$, $^1/_3$) are B′ and C at ($^1/_3$, $^2/_3$), thus implying that of the three crystallographic sites only two are equivalent. It is interesting to note at this point that an O cell packing with rigorously 3_1 chains placed at the previously specified positions can be defined so that its *c*-axis projection corresponds to the $P3_121$ projection. Such a model, in a *c*-centered lattice, requires helices of opposite chirality to be statistically present at each crystallographic position.

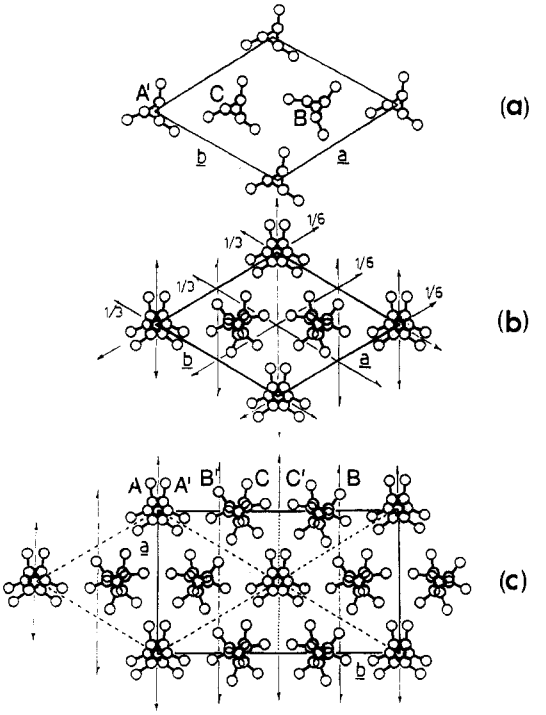

Figure 6. Schematic *c*-axis projection of a possible β-iPP packing in space groups $P3_1$ (a), $P3_121$ (b), and $C2cm$ (c). In $P3_1$ and $P3_121$, all helices are of the same chirality. Chains with a given directionality are labeled as A, B, and C, while the symmetry-related ones of opposite directionality are primed. In $C2cm$, chains of opposite chirality and of opposite directionality coexist statistically at the same crystallographic site. However, since a left-handed helix of a given directionality has an identical *c*-axis projection as a right-handed helix of opposite directionality, only two chains can be identified at each site and the projection does not vary with $P3_121$ or $C2cm$.

Figure 7 shows two electron-diffraction patterns obtained by tilting around the b* axis (which, in the trigonal case, is equivalent to *a**). The symmetry of these patterns is higher than expected for space group $P3_121$ (No. 152), as the displayed orthogonal symmetry implies $|F(hkl)| = |F(khl)|$. Scaling of the tilted data intensities confirms that, along with the very probable standard trigonal equivalencies, the relationship $|F(hkl)| = |F(kh\bar{l})|$ also holds. The electron-diffraction patterns (but also the oriented spherulitic X-ray pattern) thus display a higher symmetry than any trigonal group and suggest rather that the Laue class of the reciprocal lattice is hexagonal. However, the *hk*0 projection solution and packing symmetry considerations (vide infra) render this extremely unlikely. *While local symmetry approaches the isolated helix symmetry, i.e., $P3_1$ (no. 144; see Figure 4a), excess symmetry must arise from disorder.* Up–down disorder specified by a binary axis in the plane perpendicular to the helical axis results in the $P3_121$ symmetry (Figure 4b), *while additional reciprocal lattice symmetry implies more extensive disorder which should develop, leaving the satisfactory c-axis projection of $P3_121$ unaltered.* As far as we can see, the best way that this can be achieved is by introducing ($\bar{1}10$) or ($\bar{2}20$) mirror planes, which, for packing efficiency, are likely to have a glide component. This new symmetry element is incompatible with the 3_1 axis, and we are

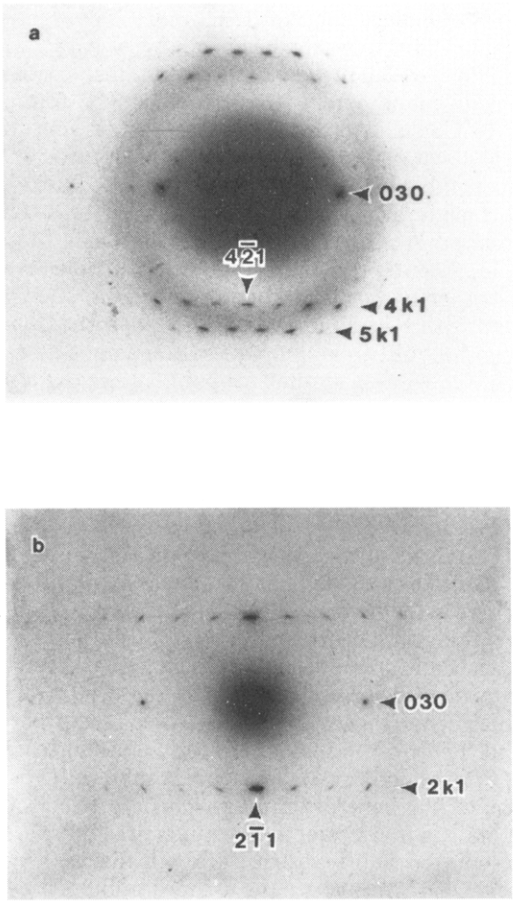

Figure 7. Electron-diffraction patterns obtained by tilting a sample around the b^* axis. Note the overall orthogonal symmetry of both patterns. Pattern (a) corresponds to an experimental tilt angle of 22°: the clearer reflections are from the 4*hkh* and the 5*hkh* zones, while the most intense *hk*0 and 6*hkh* are also observed. Pattern (b) was obtained with an experimental tilt of 42° and represents the 2*hkh* zone. All indexing is given in terms of the trigonal A cell (Figure 1).

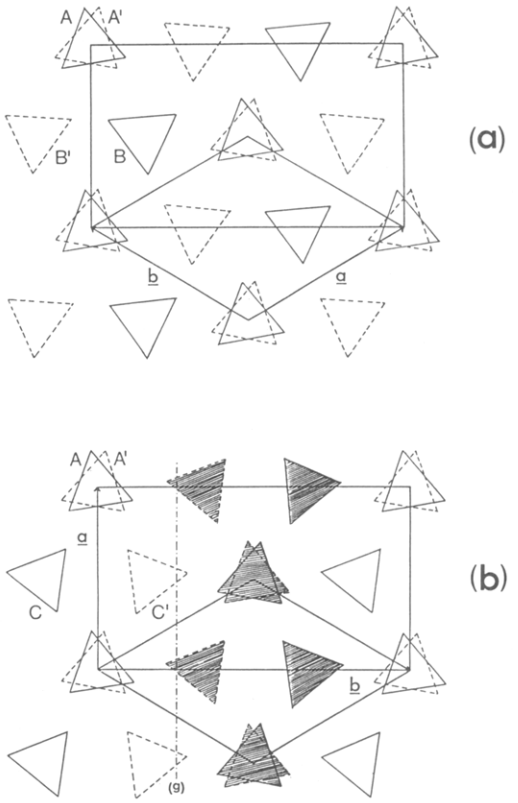

Figure 8. *c*-axis projection schemes of ordered low-energy packing models for β-iPP; triangles define the methyl carbon positions. (a) One of the most favored $P3_121$ (trigonal unit cell) arrangements with up–down statistics only at the origin: A (full lines) and A′ (opposite directionality, dashed lines) have an occupancy factor of 0.5, while B (full lines, same directionality as A) and B′ (dashed lines same directionality as A′) have an occupation factor of 1.0. Obviously all chains share the same chirality. (b) One of the lowest energy $P2nn$ (orthorhombic cell) packings: with respect to up–down statistics, similar considerations as discussed for (a) apply. Note the trilayers of chains of opposite chirality (respectively shaded and unshaded) generated by the glide plane (g).

left with the alternative of preserving the 3_1 crystallographic symmetry assuming a twinning mode defined by such a plane or eliminating the 3-fold crystallographic symmetry and implementing a trigonally microtwinned *c*-centered orthorhombic lattice (O cell, Figure 1), characterized by a glide plane perpendicular to *b* and by a 2-fold axis parallel to *a* (*a* and *b* in this case refer to the orthorhombic lattice). If we neglect for the moment the trigonal twinning, these conditions (Figure 6c), together with the *c*-projection noncentrosymmetry requirement, determine the alternative space group unequivocally as $C2cm$ (No. 40).

Reference to Figure 6c and Figure 8b is useful to point out that the statistical presence at each crystallographic site of chains of opposite chirality (in addition to the up–down type of disorder) arises because of further disorder across the plane labeled as (g) in Figure 8b. Across this plane, we can have helices either all of the same chirality or all of opposite chirality: if we always have helices of the same chirality, space group $P3_121$ results. If helices of opposite chirality were to alternate regularly across such planes, we would lose the centering and space group $P2nn$ (No. 34) would be obtained. Finally, if the two sequences were equiprobable, space group $C2cm$ would be obtained. In all these cases, the structural unit is the same: we could define it as a *trilayer of helices all of the same chirality which represents the common building block of all the three symmetries*. The analogies with the disorder models based on statistical sequences of layers of up and down chains proposed for both the α-[26,27] and the γ-iPP[4] structures should be apparent. Similar types of disorder based on domain structures of chains of opposite directionality have also been proposed for 1,4-*cis*-polyisoprene[28] and the α-phase of poly(vinylidene fluoride).[29] In the present case, while the possibility of directionality domains also exists, the distinctive feature of the disorder model is the existence of enantiomorphic domains of isochiral helices.

On a strictly crystallographic perspective, we will only note in the present communication that both the analysis of the available three-dimensional electron-diffraction data and the Rietveld analysis[30,31] of X-ray diffraction data for unidirectionally crystallized samples (see Figure 9) give nearly identical discrepancy factors close to 0.20 for space groups $P3_121$ and $C2cm$, while $P2nn$ results in a substantially worse fit (0.28). The agreement of the Rietveld analysis with electron-diffraction data is encouraging. Possible discrepancies could, however, be accounted for because the two examined samples have been crystallized under different conditions. Indeed, samples crystallized isothermally at higher temperatures are likely to be more ordered, i.e., most likely $P3_121$ or even $P3_1$. We do not want to pursue this question further in the present context, but it should be mentioned that reports concerning β_1- and β_2-structures[32] could in principle be explained in terms of the present model.

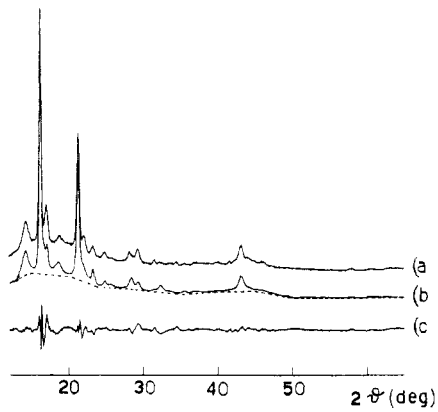

Figure 9. X-ray diffraction pattern from a film unidirectionally crystallized in a temperature gradient. The experimental spectrum is labeled as a, while the calculated diffraction pattern resulting from a prevailing β-phase contribution ($P3_121$ model) and a minor but not negligible one due to the α-modification is labeled as b. The dashed line represents the amorphous contribution and the difference spectrum is labeled c: it should be noted that some of the more prominent residual peaks in this trace correspond to either α-phase or mesophase diffraction maxima.

The essential features of the above structure analysis were confirmed by packing energy calculations that were performed following a procedure already used for α- and γ-iPP.[33] We report here preliminary results, while the full investigation will be discussed elsewhere.[34] Assuming the A cell (with three independent isochiral chains) and a fully ordered $P3_1$ symmetry, the energy per mole of trimer is 0.5 kcal higher than for fully ordered α- and γ-iPP models (space groups $P2_1/c$ and $F2dd$ or $Fd2d$, respectively). Up–down disorder can be introduced in the model crystallographically assuming either space group $P3_121$ or $P3_112$. It is interesting to note that the first choice leads to coordinates of the three independent monomers which are in essence the same as in the minimum-energy $P3_1$ structure. The energy difference between this disordered structure and the similarly disordered α- and γ-iPP structures (space groups $C2/c$ and $Fddd$, respectively) decreases to 0.3 kcal/mol of trimer. Energy minimization with the other choice, i.e., $P3_112$, leads to an energy value higher by ca. 0.2 kcal, but more surprisingly, the three independent chains in the model become practically indistinguishable, and the lattice simplifies to the one-chain subcell. It appears relevant that in the two space groups the chain axes location, the relative helical chirality, and the up–down statistics are identical: it might thus be comparatively easy for a given chain to optimize its packing with minor adjustments at the moment of crystallization or even at a later stage. It is therefore not surprising that a model with a minimal packing energy advantage is clearly preferred according to independent diffraction data. Similar reasoning can also explain why hypothetical packings with hexagonal symmetry do not occur. Such packings could be obtained by statistical substitution of differently oriented but identical isoclined 3_1 helices at the same crystallographic site. Assuming that locally nonequivalent arrangements could exist, the less stable ones should easily transform to the more favored ones, thus causing the loss of hexagonal symmetry. Alternatively, apparent hexagonal symmetry could result from appropriately oriented isochiral microtwins, but considerations similar to the preceding ones may also suggest this hypothesis to be unlikely.

One of the more important issues resulting from the preceding discussion of the diffraction data is whether the coupling across the specified glide plane (see Figure 8b) of domains of helices of opposite chirality is energetically acceptable. This question has been investigated for space group $P2nn$, which presents in a regular fashion the same local glide plane arrangement that can be found statistically in $C2cm$. According to our results, if full statistical up–down disorder is assumed, that symmetry leads to unacceptably high energy values. On the contrary, taking into consideration only chains A and C and the symmetry-related A′ and C′ (see Figure 8b), i.e., only selected arrangements, the energy can be as little as 0.6 kcal/mol of trimer higher than for the minimum energy packing found with $P3_121$ symmetry. Models with $C2cm$ symmetry can be built in which this arrangement has a probability of 0.5 while a similar probability exists for a $P3_121$-type packing. As a consequence, the average "excess energy" with respect to the minimum $P3_121$ value would be only 0.3 kcal/mol of trimer. Similar or greater differences are found between fully ordered and up–down statistically disordered structures in α- and γ-iPP.[26,33]

A detailed analysis of disorder is beyond the scope of this article. Suffice it to state at present that identical occupancy factors for A, B, and C chains may represent a first approximation. With such a model, reference to Figure 8 suggests an explanation for the pattern of diffuse diffracted intensity streaks characterizing the $hk0$ electron-diffraction patterns (Figure 2). These streaks run perpendicular to the b^* direction, which can be assumed to coincide in the trigonal and the orthorhombic lattices, and (because of the centrosymmetry of the diffraction pattern and its trigonal projection symmetry) superpose into the six-pointed star pattern. We will discuss this feature briefly with reference to the orthorhombic lattice, neglecting in the first step of our analysis the trigonal symmetry of the projection. Examination of Figure 6c shows that the projection of the structure on a (i.e., along b) is substantially less disordered than on b (i.e., along a). Specifically, while chains A and A′ have identical projections on a but not on b, this observation only holds approximately for the other chains except if B and B′ and/or C and C′, respectively, appear in pairs (see, e.g., Figure 8a and 8b): in such cases, it is again strictly valid. The streaks are thus consistent with our model of a substantially greater amount of disorder along b: as the b^* axis is intersected by the diffuse intensity where the systematically absent 030 reflection would be found, we can conclude that disorder is particularly significant at this level, i.e., it arises from first-neighbor interhelical interactions. As the trigonal projection symmetry implies that the streaks also intercept the a^* axis (at the 200 reflection, i.e., again at the level of first-neighbor interactions), the reasoning becomes somewhat more complex but without providing any additional clarification to the model.

Conclusions

A clear result of the present analysis is the confirmation of the conjecture[11,13] that iPP 3_1 helices pack in the pseudohexagonal β-modification in isochiral domains. The important novelty, aside from a detailed structural description, is that these domains combine, coherently or incoherently, via glide-plane symmetry elements (the 200 or the equivalent 220 planes of the trigonal cell A), giving rise to an overall statistical coexistence of R and S helices at the same crystallographic site (see Figure 10). *If adjacent domains of opposite chirality interact incoherently (twinning), the result is the trigonal space group $P3_121$ while coherent combination across the mentioned glide planes affords the $C2cm$ orthorhombic symmetry*

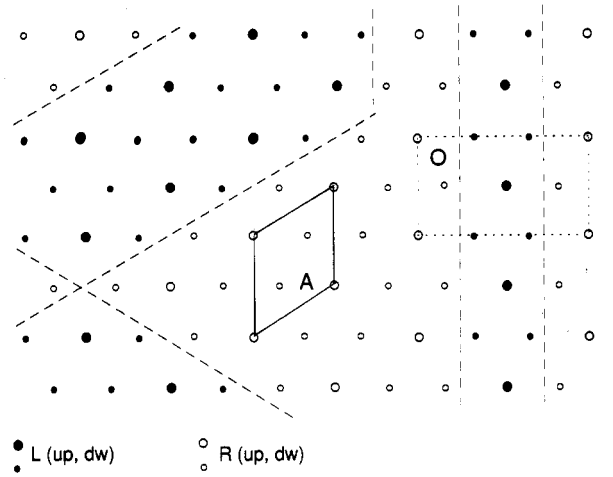

Figure 10. Possible domain structure for β-iPP. Large circles represent the origin chain in the trigonal system (and possibly the equivalent centered one on the orthorhombic lattice). Small circles stand for the other two, symmetry-related chain positions. The dashed lines indicate possible isochiral domain borders. Notice the trilayer structure at the right. The displayed O unit cell presents local *P2nn* symmetry. In principle, different domains can scatter either incoherently or coherently. In the former case, trigonal symmetry applies, while in the latter orthorhombic symmetry results.

and leads to the disruption of crystallographic trigonal symmetry. The "hexagonal" reciprocal lattice symmetry can be satisfactorily accounted for by both of these models (for the orthorhombic case, trigonal microtwinning is required) *which differ in fact very marginally*, except in a strictly crystallographic perspective. It is thus not at all surprising that the crystallographic refinement of either leads to very similar, acceptable results. Packing energy calculations confirm the possibility of both of the above arrangements.

It should be recalled that twinning is not required by the symmetry of *hk*0 data but results from the tilted-crystal electron-diffraction patterns. We cannot exclude that a more ordered untwinned form will develop under appropriate crystallization conditions. A structure based on *small isochiral domains which can interact favorably with domains of opposite chirality* is less complex or erratic than could seem at first: in fact, the chirality of the domains can justify the occurrence of a third crystalline polymorph of iPP, the β-phase, which would be hardly understandable if it did not display major differences with respect to the α- and γ-crystalline modifications in which helices of both chiralities coexist. Furthermore, it should be noted that the high growth rate of β-iPP is hardly compatible with the existence of large crystals built with helices all sharing the same chirality: entities of that kind would require either unmixing of helices of opposite chirality or major conformational rearrangements of helix fragments from a given chirality to the opposite one, resulting in large assemblies of isochiral helices. Such events would be difficult to account for with an achiral molecule as isotactic polypropylene and, in any case, should be kinetically less favored than cocrystallization of helices of opposite chirality. These conceptual objections are largely eliminated by the present model of small (coherent or incoherent) isochiral domains. We notice that somewhat similar models, involving coupling of domains of opposite chirality, e.g., through twinning, are likely to occur whenever a chiral crystalline phase is obtained with a nonchiral macromolecule.

While the details and the dimension of the domain structure in the present case are still under investigation and largely depend on the specific sample, we are quite confident that the essential features of the β-iPP structure are now clarified. It should be stressed that indeed all available data are accounted for by the present structure: (i) It is hardly surprising that a melting–recrystallization process is required to transform a β-specimen into an α-specimen because of the basic differences between the two structures. (ii) The lower melting point of the β-modification is consistent with the slightly higher packing energy and the domain structure of this modification. (iii) The instability of β-iPP with respect to drawing can be rationalized, as tensile strain tends to favor denser packing and disrupts clear boundaries between domains of helices of opposite chirality. At low enough temperatures, this results in recrystallization into the mesophase, which apparently is characterized by poorly ordered coexistence of helices of both chiralities combining features of both the α- and β-modification.[16] (iv) Planes separating adjacent domains are orthogonal to the growth direction (i.e., a^* of the A cell), in line with reasonable crystal growth mechanisms.

Finally the discussed disorder models are particularly relevant to recent morphological investigations[35] of β-iPP crystals which indicate that β-lamellae fracture in a rather regular fashion simply upon annealing. On the basis of our structural model, it would be reasonable to suggest that the fracture surface must be perpendicular to the b^* axis and in essence parallel (or at 120°) to the growth faces of the original quasi-hexagonal lamellae. The quoted paper[35] and other very recent investigations[36] also lend additional support to the idea that β- and α-iPPs can also exist within the same spherulite.

Acknowledgment. We express appreciation for stimulating discussions with Dr. Arturo Colombo and Professor Giuseppe Allegra. We also thank Professor H. D. Keith for participating in the difficult tilted-crystal electron-diffraction experiment. Significant portions of the investigation were carried out in 1991 while S.V.M. was at Case Western Reserve University supported by a NATO Advanced Fellowship.

Note Added in Proof. Similar structural conclusions about β-iPP have also been reached in a parallel investigation by Kopp, Dorset, and Lotz[37] using direct electron-crystallographic techniques.

References and Notes

(1) Natta, G.; Corradini, P. *Nuovo Cimento Suppl.* **1960**, *15*, 40.
(2) Brückner, S.; Meille, S. V. *Nature* **1989**, *340*, 455.
(3) Turner-Jones, A.; Aizlewood, J. M.; Becket, D. R. *Makromolek. Chem.* **1964**, *75*, 134.
(4) Meille, S. V.; Brückner, S.; Porzio, W. *Macromolecules* **1990**, *23*, 4114.
(5) Lotz, B.; Graff, S.; Straupe, Ch.; Wittmann, J. C. *Polymer* **1991**, *32*, 2017.
(6) Brückner, S.; Meille, S. V.; Petraccone, V.; Pirozzi, B. *Prog. Polym. Sci.* **1991**, *16*, 361.
(7) Norton, D. R.; Keller, A. *Polymer* **1985**, *26*, 704.
(8) Keith, H. D.; Padden, F. J.; Kissel, W. J.; Wyckoff, H. W. *J. Appl. Phys.* **1959**, *30*, 1485.
(9) Addink, E. J.; Beintema, J. *Polymer* **1961**, *5*, 185.
(10) Geil, P. H. *J. Appl. Phys.* **1962**, *33*, 642.
(11) Turner-Jones, A.; Cobbold, A. J. M. *J. Polym. Sci.* **1968**, *6*, 539.
(12) Fujiwara, Y. *Kolloid Z.-Z. Polym.* **1969**, *226*, 135.
(13) Samuels, R. J.; Yee, R. Y. *J. Polym. Sci., A2* **1972**, *10*, 385.
(14) Hsu, C. C.; Geil, P. H. *J. Polym. Sci., Polym. Phys. Ed.* **1986**, *24*, 2379.
(15) Grubb, D. T.; Yoon D. Y. *Polym. Commun.* **1986**, *27*, 84.
(16) Corradini, P.; Petraccone, V.; De Rosa, C.; Guerra, G. *Macromolecules* **1986**, *19*, 2699.
(17) Corradini, P.; De Rosa, C.; Guerra, G.; Petraccone, V. *Polym. Commun.* **1989**, *30*, 281.

(18) Yan, R. J.; Li, W.; Li, G.; Jiang, B. *J. Macromolecular Sci. Phys.* **1993**, *B32*, 15.
(19) Gomez, M. A.; Tanaka, H.; Tonelli, A. E. *Polymer* **1987**, *28*, 2227.
(20) Leugering, H. J. *Makromolek. Chem.* **1967**, *109*, 204.
(21) Crissmann, J. M. *J. Polym. Sci., Polym. Phys. Ed.* **1969**, *7*, 389.
(22) Lovinger, A. J.; Chua, J. O.; Gryte, C. C. *J. Polym. Sci., Polym. Phys. Ed.* **1977**, *15*, 641.
(23) Leugering, H. J.; Kibsch, G. *Angew. Makromolek. Chem.* **1973**, *33*, 17.
(24) Dragaun, H.; Hubney, H.; Muschik, H. *J. Polym. Sci., Polym. Phys. Ed.* **1977**, *15*, 1779.
(25) Campbell Smith, P. J.; Arnott, S. *Acta Crystallogr.* **1978**, *A34*, 3.
(26) Corradini, P.; Giunchi, G.; Petraccone, V.; Pirozzi, B.; Vidal, H. M. *Gazz. Chim. Ital.* **1980**, *110*, 413.
(27) Corradini, P.; Petraccone, V.; Pirozzi, B. *Eur. Polym. J.* **1983**, *19*, 299.
(28) Natta, G.; Corradini, P. *Angew. Chem.* **1956**, *68*, 615.
(29) (a) Takahashi, Y.; Tadokoro, H. *Macromolecules* **1983**, *16*, 1880. (b) Bachmann, M. A.; Lando, J. B. *Macromolecules* **1981**, *14*, 40. (c) Takahashi, Y.; Matsubara, Y.; Tadokoro, H. *Macromolecules* **1983**, *16*, 1588.
(30) Rietveld, H. M. *J. Appl. Crystallogr.* **1969**, *2*, 65.
(31) Immirzi, A. *Acta Crystallogr.* **1980**, *B36*, 2378.
(32) Shi, G.; Zhang, X.; Cao, Y.; Hong, J. *Makromol. Chem.* **1993**, *194*, 269.
(33) Ferro, D. R.; Brückner, S.; Meille, S. V.; Ragazzi, M. *Macromolecules* **1992**, *25*, 5231.
(34) Ferro, D. R.; Brückner, S.; Meille, S. V. Manuscript in preparation.
(35) Rybnikar, F. *J. Macromolec. Sci. Phys.* **1991**, *B30*, 201.
(36) Fillon, B.; Thierry, A.; Wittmann, J. C.; Lotz, B. *J. Polym. Sci., B, Polym. Phys.* **1993**, *31*, 1407.
(37) Kopp, S.; Dorset, D.; Lotz, B. *Bull. Am. Phys. Soc.* **1994**, *39*, 108; *C. Rendus* (submitted).